From geomagnetic observations at COI to GICs in the Portuguese power system network

Fernando Pinheiro[1a], Joana Ribeiro[2], M. Alexandra Pais[1b], Paulo Ribeiro[3], Anna Morozova[1c], Fernando M. Santos[4], João Fernandes[5] & Cristiana Francisco[1d]

[1] University of Coimbra, CITEUC - Centre for Earth and Space Research of the University of Coimbra, Faculty of Sciences and Technology, Department of Physics, Rua Larga 2, P-3004 516 Coimbra, Portugal. E-mail: [a]fjgpinheiro.astro@gmail.com; [b]pais@fis.uc.pt; [c]annamorozovauc@gmail.com; [d]filipafrancisco24@gmail.com

[2] University of Coimbra, IDL - Instituto Dom Luiz, Faculty of Sciences and Technology, Department of Physics, Rua Larga 2, P-3004 516 Coimbra, Portugal. E-mail: jaribeiro@uc.pt

[3] University of Coimbra, CITEUC - Centre for Earth and Space Research of the University of Coimbra, Geophysical and Astronomical Observatory, Almas de Freire - Santa Clara, P-3040 004 Coimbra, Portugal. E-mail: pribeiro@ci.uc.pt

[4] University of Lisbon, IDL - Instituto Dom Luiz, Faculty of Sciences, Campo Grande, P-1749 016 Lisbon, Portugal. E-mail: fasantos@fc.ul.pt

[5] University of Coimbra, CITEUC - Centre for Earth and Space Research of the University of Coimbra, Faculty of Sciences and Technology, Department of Mathematics, Apartado 3008, EC Santa Cruz, P-3001 501 Coimbra, Portugal. E-mail: jmfernan@mat.uc.pt

Abstract: Geomagnetic storms induce electric fields on the ground, which are the source of Geomagnetically Induced Currents (GICs) in grounded conductors such as transmission power systems. Despite being a phenomenon more often associated with countries located at high latitudes, they are not exclusive to them. Indeed, there are accounts of GICs in low latitude countries such as China, South Africa, Brazil or Spain. In this work we will provide a quick overview of Space Weather and Geomagnetism, indicating the sources of variability of Earth's magnetic field. Moreover, we will show how to compute the electric fields generated by geomagnetic storms and the GICs that are induced in transmission power grids. We use as an illustrative example the case of the southern Portuguese power network. Our study is made within the framework of MAG-GIC project, which

Abrantes, I., Callapez, P. M., Correia, G. P., Gomes, E., Lopes, B., Lopes, F. C., Pires, E., & Rola, A. (Eds.), *Uma visão holística da Terra e do Espaço nas suas vertentes naturais e humanas. Homenagem à Professora Celeste Romualdo Gomes*. Coimbra: CITEUC.
 DOI: http://doi.org/10.5281/zenodo.4409272

aims to characterize GICs in the whole Portuguese transmission power system network. The calculations are based on observations from the magnetic observatory of Coimbra, for which a short description is given.

Keywords: Geomagnetic induced currents, Geomagnetic storms, Magnetic observatory of Coimbra, Magnetotellurics, Southern Portuguese power system network, Space Weather.

Resumo: *A atividade solar é responsável por tempestades geomagnéticas que, de tempos a tempos, se fazem sentir à superfície da Terra com indução de campos elétricos na crosta e manto superior. Tais campos estão na origem de correntes elétricas induzidas em infraestruturas de materiais condutores que se estendem ao longo de grandes distâncias, com ligação à terra, tal como as redes de transporte de energia elétrica. Essas correntes são designadas por* Geomagnetically Induced Currents *(GICs). Apesar de se tratar de um fenómeno com maior impacto em países a latitudes elevadas, estudos recentes mostram que as GICs são também observadas nas redes de transporte de eletricidade de países a latitudes baixas e intermédias. É o caso da China, África do Sul, Brasil ou Espanha. Neste artigo começamos por introduzir a área de estudo da Meteorologia Espacial e explicar a importância das variações do campo geomagnético como motor das GICs. Em seguida, expomos as diferentes etapas do cálculo de GICs na rede elétrica, mostrando como chegar a estimativas de valores que podem ser testadas experimentalmente. Utilizaremos como exemplo de aplicação a rede elétrica nacional na região Sul de Portugal, uma parte do estudo que desenvolvemos no âmbito do projeto MAG-GIC e que se estenderá à totalidade da rede nacional. As estimativas obtidas têm por base os registos do sinal de campo geomagnético no observatório magnético de Coimbra, pelo que faremos um apanhado dos mais de 150 anos de atividade deste observatório.*

Palavras-chave: *Correntes geomagnéticas induzidas, Tempestades geomagnéticas, Observatório Magnético de Coimbra, Magnetotelúricos, Rede elétrica do Sul de Portugal, Meteorologia Espacial.*

Introduction

Space Weather (SW) is a field of Science that crosses Solar Physics with Aeronomy and Geomagnetism, dealing with the impact of solar radiation and solar wind with the Earth. This is definitively not a new subject. As an example, we can point out the 1905 paper by Walter Maunder (the same “of” the famous solar minimum) where we can read that “(…) our magnetic disturbances are due to a solar action, taking place along definite lines, some of which strike the Earth, and some of which do not (…)”.

It is well known that SW events can have consequences in several technological-based economic sectors, such as the Global Navigation Satellite System, communication and power grid systems. So SW studies raised the interest not only from pure science researchers, in order to understand the physical mechanisms involved, but also from engineers, to predict the consequences of space weather events for social and economic activities.

Although it is still not clear the real economic impact of SW events, because most of the time the information from the end-users is lacking (Eastwood et al., 2017), some estimations have been done. If an extreme case event, as the Carrington Event in 1859 (one of the largest geomagnetic storms

observed to date, from an intense ejection of solar coronal material) occurred today, it would cause damages to the UK's grid system with costs of around 16 billion pounds. Such a high impact could be largely reduced if mitigation mechanisms were in operation (Oughton et al., 2019). This same kind of event would have an impact of about 6% (over a year) in North America's gross domestic product (Oughton, 2018). Schrijver et al. (2014) analysed 11,242 complaints (reported to insurance companies) for malfunctioning of electrical networks between 2000 and 2010, in the USA: these complaints increased in days of intense geomagnetic activity. These facts have led the insurance sector to start considering SW hazard as a potential threat.

Space Weather phenomena are mostly observed at high latitudes (Pulkkinen et al., 2012). However, during the last years several studies show that significant effects of SW at mid-low latitudes cannot be ruled out (e.g. Torta et al., 2017). This work focus on one particular consequence of SW events: Geomagnetically Induced Currents (GICs) on high voltage power networks.

Fast geomagnetic variations induce electric fields on the ground, which on their turn induce electric currents travelling along grounded conductors (the GICs) such as telegraph lines (as known since the late XIX century), pipelines or high voltage power networks (e.g., Pirjola, 2002). While the impact of GICs on pipelines can be seen through an increase of the galvanic corrosion, in the case of electric power network systems the impact can be felt through the introduction of harmonics in the electric signal, the saturation of the transformers' cores (with loss of reactive power), damage of transformer windings or the overheating of transformer insulating fluid (Molinski, 2002). Ultimately, these problems can result in the irreversible damage of power transformers and blackouts over wide regions, like the Hydro-Québec's power system blackout on the 13th March 1989, which left 7 million people without electricity for nine hours.

In this paper, we explain how to compute GICs in a power system network. As an illustrative example, we present the case of the southern Portuguese power network. The results shown here were obtained in the framework of project MAG-GIC (PTDC/CTA - GEO/31744/2017), the first effort to produce realistic estimates of GICs in the national power lines.

The magnetic observatory of Coimbra

The magnetic observatory of Coimbra (COI) has been monitoring the Earth's magnetic field for more than 150 years, producing useful data for different studies, from the characterization of 'jerks' (i.e. sudden changes in the linear trend of geomagnetic field time variations), that originate inside the Earth (e.g. Pais & Miranda, 1995; Morozova et al., 2014), to effects of magnetospheric currents at mid-latitudes (Castillo et al., 2017) and the present study of GICs estimation in the Portuguese transmission power system network (Alves Ribeiro et al., 2020). It is the only magnetic observatory in mainland Portugal to measure and record the geomagnetic field variations in a continuous mode, as well as being amongst the oldest observatories in the global network of the International Association of Geomagnetism and Aeronomy (IAGA).

The long instrumental records from the geomagnetic field components at COI provide valuable information about the variability of geomagnetic elements and indices, their trends and cycles, and can be used to improve our knowledge on the sources that drive variations of the geomagnetic field: liquid core dynamics (internal) and solar forcing (external). However, during its long lifetime, inevitable changes of the instruments, measurement procedures and even re-location of the observatory took place, with consequent interruptions and or periods of less data quality (Morozova et al., 2014). Two distinct working periods can be identified on the basis of two different operating sites: the first period extends from the observatory's foundation in 1864 to its relocation in 1932 and refers to the Cumeada site; the second period extends from 1932 to the present and refers to the second site Alto da Baleia.

The increasing urbanization during the first quarter of the 20th century, particularly the installation in 1929 of a new tram line only 50 m away from the variographs' house, dictated the re-location of the magnetic observatory to its current site (Alto da Baleia) in 1932. Nonetheless, the first years in Alto da Baleia suffered from a very flawed operation and all observations ended up being interrupted around 1941 due to the difficult years of World War. The oversimplification of observation routines and the non-negligible perturbations mainly related to the ageing and drift of old absolute instruments that were kept in use, as well as the likely lack of experience in the operation of the newly acquired Askania variographs, can be regarded as the main reasons for the low quality of data during the first 20 years in Alto da Baleia (1932-1951).

Magnetic observatory routines were resumed nearly the end of 1951 on a methodical and more accurate basis. The construction of a new house of absolute observations combined with the use of new absolute instruments (QHM, BMZ, Askania Declinometer) and the reinstallation of the Askania variographs allowed to obtain series of good quality for more than three decades (~ 1951-1980s) (Pais & Miranda, 1995; Ribeiro & Pais, 2004; Morozova et al., 2014). By the late 1980s, the COI data began showing again some non-negligible perturbations mainly related to the ageing and drift of instruments. Part of these problems and limitations were overcome in 2007 by replacing the complete old set of instruments with a modern digital fluxgate variometer (a DMI model FGE, suspended version) and a standard pair of absolute instruments (a DI-flux based on a Bartington fluxgate MAG01H sensor mounted on a MG2KP Theodolite and an Overhauser GSM-90F1 scalar magnetometer). This upgrading resulted in a healthier baseline stability and in a clear quality improvement of the monthly and annual data series as demonstrated by the lowering variance of their first time-differences (Morozova et al., 2014). Inevitably, the ongoing city growth continues to threaten the good functioning and quality of observatory data. To overcome this, a new relocation of the Coimbra's observatory to a rural area near about 20 km from Coimbra center is underway.

Geomagnetic field variations

The observed geomagnetic field is a mix of contributions from different sources, some acting on a periodic or quasi-periodic basis (daily variation, solar cycle variation), others showing very irregular

behaviour (geomagnetic storms) and still others with a short-term smooth behaviour with trends that change from time to time (main field variation) (e.g. Yamazaki & Maute, 2017). From the three components above, only the geomagnetic storm field contributes significantly to GICs, because of its higher frequency content. It can in fact be shown analytically, for a simple half-space conductivity model, that induced currents are proportional to dB/dt (e.g. Pirjola, 2002). Nonetheless, and to better contextualize the GIC calculation, a short account is given on different contributions to geomagnetic field variability.

Internal field sources

In addition to a relatively small contribution from magnetized minerals in the crust, the Earth's geomagnetic field component with primary sources inside the solid planet, is due to convective motions within its outer metallic core. The electric currents induced by the motion of the conducting fluid relative to the mean magnetic field create new, regenerating field, through a dynamo mechanism. The nature of this mechanism implies that the geomagnetic field is not static; its orientation and intensity change on timescales of several months to years and centuries (e.g. Hulot et al., 2015). Occasionally, this secular variation presents sudden changes on its evolution known as geomagnetic jerks, where the rate of change goes from an increase to a decreasing trend or vice-versa (e.g. Mandea et al., 2010). A good example of jerks can be seen in the sudden and recent changes in Earth's magnetic poles displacement. On a longer timescale, magnetic reversals resulting from the geodynamo can be seen in several geological layers, with no particular periodicity.

Using data from the global network of on-Earth observatories as well as from satellite missions as the most recently Swarm constellation, spherical harmonic models for the core field can be computed. Their spatial resolution will hardly decrease below ~1600 km (since for shorter length-scales the crustal field dominates) and the most rapid internal time changes possibly detected are of the order of ~1 year (smaller periodicities are hampered by the external field temporal variability) (see e.g. Finlay et al., 2017).

Daily variation

The Sun is the source of magnetic field variations seen on Earth on much shorter timescales, from several days to minutes. The Sun irradiates our atmosphere, heats and ionizes the air at high altitudes generating most of the mesosphere and thermosphere winds, waves and tides. The partially ionized area of the Earth atmosphere from ~70 km to ~1000 km is called the ionosphere. At the altitude of ~90-150 km, an electric current system is generated in the sunlit hemisphere, in the so-called E dynamo region. The main drivers for these currents are the main geomagnetic field and winds and waves in the neutral atmosphere, as, for example, the tidal wave (-1.2) symmetrical to the equator and with a period of 24 h (see Amory-Mazaudier, 2009, for details). The electric current system that

originates in the daily heating of the atmosphere consists of two vortices quasi-symmetrical to the equator, with anti-clockwise (clockwise) electrical currents in the Northern (Southern) Hemisphere. In turn, these vortices produce a magnetic field of the order of a few nT measured on the ground. The focuses of these vortices are located in the latitude range of 30-40º depending on the longitude and hemisphere. As the day progresses, the position on the globe of these vortices moves westward following the Sun. Thus, for any fixed location on the planet, the geometry of the system changes along the day returning to a similar condition after one day. The variation of the geomagnetic field associated with this current system is called the solar (= daily) quiet (= not related to geomagnetic disturbances) variation or Sq. The process of the generation of the Sq geomagnetic field variations is schematically shown in figure 1.

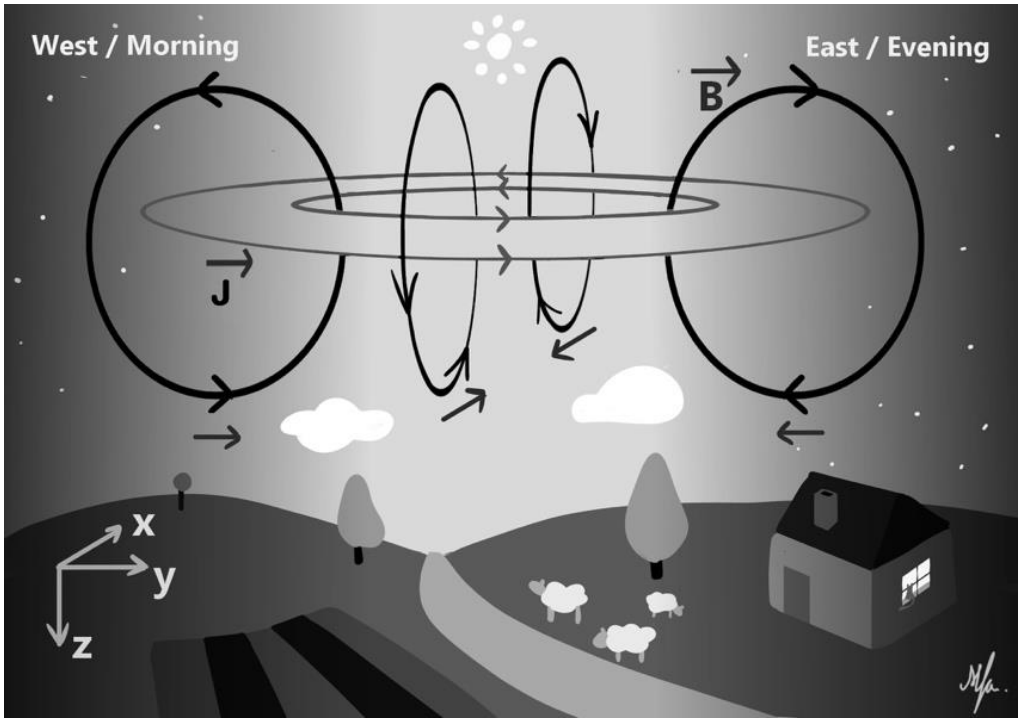

Figure 1 - Generation of the Sq B field by the ionospheric vortex, at the Northern Hemisphere. Horizontal lines represent electric current lines. Vertical lines represent the magnetic field generated by the current system. [Credits: K. Morozova]

The typical curve of the measured quiet daily variations of the geomagnetic field on the ground depends on the position of a geomagnetic observatory or station relative to the vortex (Chapman & Bartels, 1940; Amory-Mazaudier, 2009). Figure 2 shows variations of the geomagnetic (B) (and electric, E) components B_x (E_x) (along the X-axis, positive in the direction to the geographic North, see Fig. 1) and B_y (E_y) (along the Y-axis, positive in the direction to the geographic West) generated by an ideal vortex (with symmetry axes along the central meridian and central parallel) in the Northern Hemisphere, for a station located to the north of the vortex focus. As one can see, observed B_x variations are symmetrical around the local noon, while B_y variations related to Sq are antisymmetrical.

The change of curvature sign of the B_x-Sq curve (does B_x have minimal or maximal values around the local noon) takes place around the foci latitudes: for stations to the north (south) of the vortex focus in the Northern Hemisphere B_x-Sq variation shows a minimum, and for stations located between the two foci, the B_x-Sq curve shows a maximum. The curvature sign of the B_y-Sq curve changes near the equator.

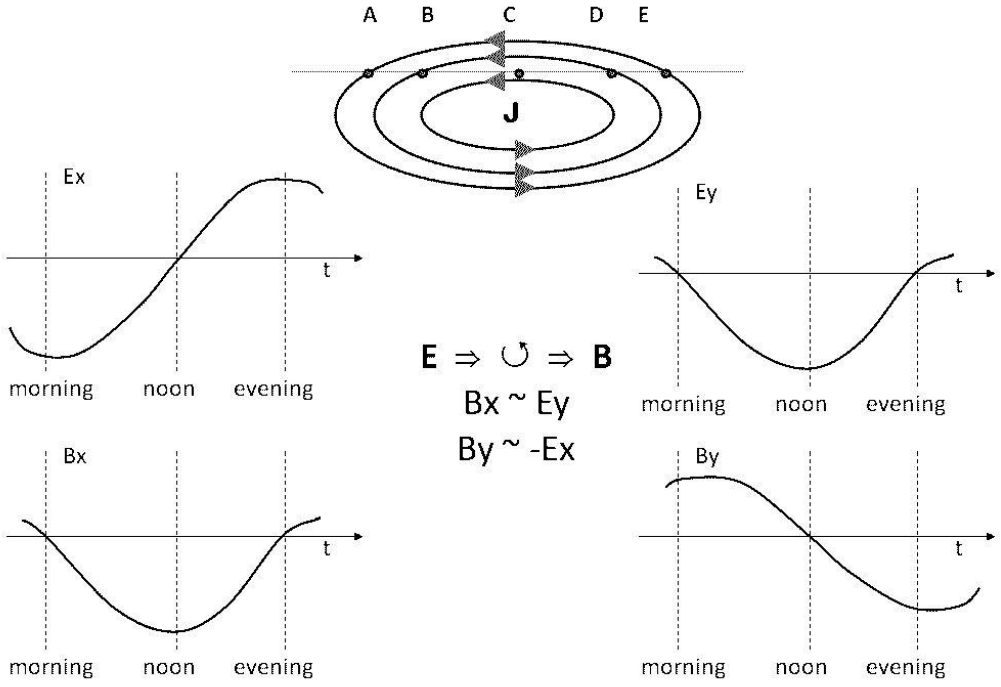

Figure 2 - Daily variation of the electric and magnetic field components along X and Y axis caused by an ideal Sq vortex in the Northern Hemisphere for a station located to the north of the vortex focus. Arrows show the direction of the current J (and of the electric field E).

Since the Earth's rotation axis is not perpendicular to the ecliptic plane, the Northern (Southern) hemisphere receives more sunlight in June (December) and less in December (June). These changes result in seasonal variation of the Sq amplitude and position of the vortex foci. In general, the daily amplitude of Sq is higher (lower) and the focus mean latitude is lower (higher) during the local summer (winter) season. There are other sources for the Sq day-to-day variability. One of them is the variability of conditions in the upper atmosphere: regular, daily and seasonal, and irregular variation in the waves and tides amplitude and amplitude and direction of the thermospheric winds. Solar flares, short-living increases of the solar UV and X irradiance as well as strong bursts of the solar radio flux can dramatically increase the ionization level of the sunlit upper atmosphere affecting ionospheric conductivity and related current systems and magnetic field variations. Another source for Sq variability are geomagnetic disturbances (geomagnetic storms and substorms) resulting in perturbations of the polar ionosphere which, in turn, propagate to the lower latitudes changing the shape, position and intensity of ionospheric current systems, including the Sq one. For regions close

to the equator, another important structure in the Earth upper atmosphere is the equatorial electrojet, an eastward flow of charged particles along the geomagnetic equator, which significantly affects ionospheric conditions, and the shape and the amplitude of the Sq variation.

An approach considered at the moment as the standard one to estimate Sq from observations consists of the selection of days with lowest level of geomagnetic field perturbations (so called “quiet days”, typically, 5 days per month) and averaging of the observed daily geomagnetic field variations observed at a particular geomagnetic observatory or stations over selected days. Still there are a number of other methods to extract Sq variations from the observational data (see e.g. Yamazaki and Maute, 2017, for a review). All methods have their pluses and minuses and the choice of a method depends on the data availability and study goals.

Geomagnetic storms

During geomagnetic storms, variations of the magnetic field are much more irregular. These variations result from interactions between the magnetosphere and the solar wind (e.g. Koskinen, 2011). Despite being known since the beginning of the XIX century (discovered by A. von Humbolt in 1806), it took nearly fifty years to discover their origin (Gauss had correctly guessed that their source lied outside the solid planet).

The answer came with the largest geomagnetic storm ever recorded, when a massive coronal mass ejection (CME) hit our planet between the 1st and 2nd of September 1959, the Carrington Event. This event made clear the existing connection between geomagnetic storms and solar activity. As in the case of the Carrington Event, the strongest geomagnetic storms are associated with CMEs, while the less intense storms can be driven by strong solar winds from coronal holes. In general terms, a geomagnetic storm can be described in the following way (see e.g. Gonzalez et al., 1994): an initial increase of solar wind pressure and density compresses the portion of magnetosphere facing the incoming wind, resulting in a momentary increase of the field’s strength in a matter of minutes. This phase is known as the storm sudden commencement. The main phase follows, during which charged particles, that entered the magnetosphere and ionosphere along the magnetic field lines, give rise to electric currents that in general result in a relatively fast weakening of the geomagnetic field. Finally, as its name suggests, during the recovery phase, the magnetic field returns to its initial condition over several hours that can amount to a few days (as seen in Fig. 3).

Real cases can be more complex than this. A geomagnetic storm may not have a sudden commencement or, as the properties of the solar wind and interplanetary medium change, the storm can be divided into several substorms. Likewise, the orientation of the interplanetary magnetic field (IMF) with respect to the Earth’s dipole field has an impact on the amount of charged particles that may enter the magnetosphere. The interplanetary magnetic field can be decomposed into three cartesian components: one in the Sun-Earth direction (IMFx); other in the direction perpendicular to the plane containing the Sun-Earth line and the Earth’s magnetic dipole (IMFy) and the third one

perpendicular to the other two (IMFz). The IMFz sign is generally considered a good proxy for the probability of particles from the solar wind entering the magnetosphere and causing geomagnetic storms.

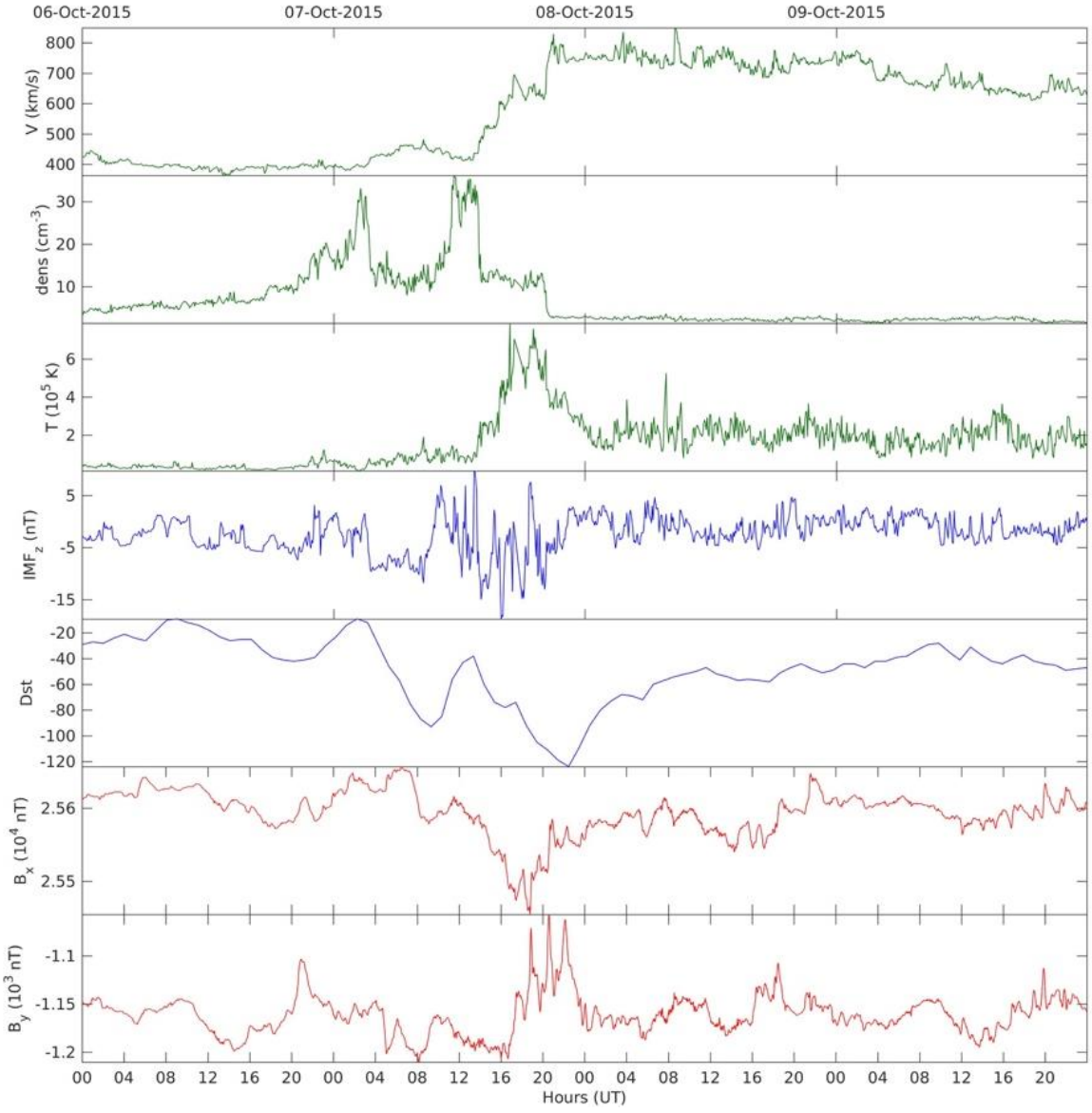

Figure 3 - For the time interval between the 6th and 10th of October 2015 and from top to bottom, 1-minute values of solar wind properties (velocity V, proton number density Np and temperature T, in green) and of IMFz (top blue curve), all obtained from the OMNI database. The fifth-row plot is for hourly values of the Dst geomagnetic index (blue curve) and the two bottom plots are 1-minute values of the horizontal components of the geomagnetic field (Bx and By, in red) recorded at COI [Source: Francisco, 2020].

As charged particles enter the magnetosphere and ionosphere, they originate different electric currents. For instance, particles trapped in the Van Allen Radiation Belts originate a ring current around the planet. Likewise, the deflection of charged particles in the magnetopause (the boundary between the magnetosphere and the surrounding plasma) results in electric currents around the polar

cusps (Fig. 4). A more detailed description of these currents and others can be found in the work of Ganushkina et al. (2018). Different models attempt to simulate the magnetic signal from the ionospheric and magnetospheric current systems with different degrees of success. The Tsyganenko & Sitnov (2005) or the BATS-R-US (Glocer et al., 2013) are just two examples of numerical models, the former semi-empirical and the later physically based. Figure 5 shows results of these simulations for the 7th October 2015 geomagnetic storm. Notice the good performance of the TS05 model in predicting this storm, in particular, especially with respect to the Bx component in agreement with results from Castillo et al. (2017). As pointed out in that study, FAC and partial ring currents are most important to explain both the time variability during the storm and the magnetospheric daily variation.

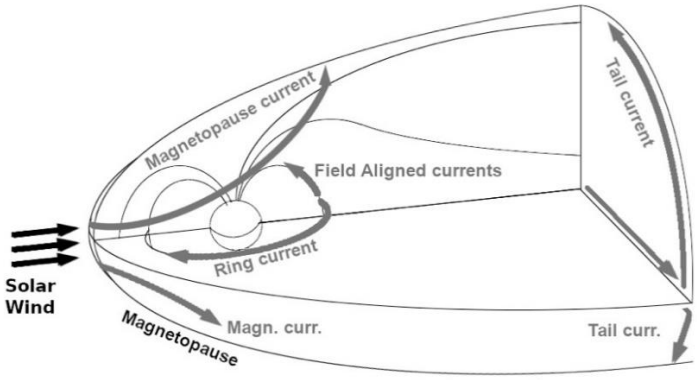

Figure 4 - Earth's magnetosphere and the main magnetospheric currents.

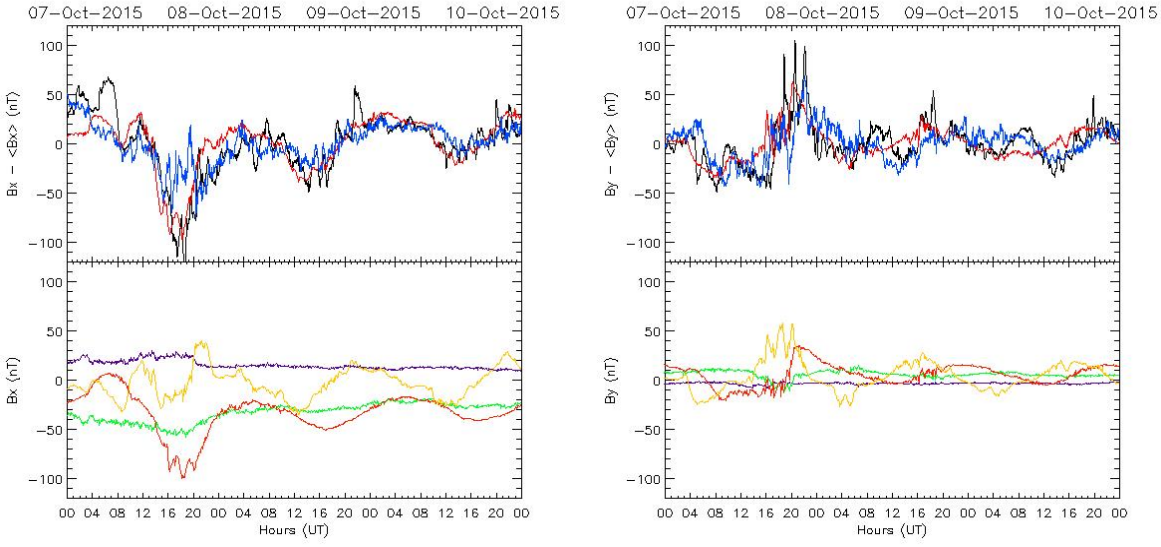

Figure 5 - Top: comparison between Bx (left) and By (right) components of the geomagnetic field recorded at COI and the corresponding simulations of the TS05 (red) and BATS-R-US (blue) models, for the geomagnetic storm of the 7th October 2015. Bottom: contribution from the magnetopause (blue), tail (green), field aligned (yellow) and symmetric plus partial ring (orange) magnetospheric currents, to the total estimated field using the TS05 model. All curves show 5-min values.

Geomagnetic storms can have different outcomes. The most notorious are the planetary Auroras. In the case of the Carrington Event, auroras were seen at latitudes as low as that of the Caribbean sea. But GICs can also be very significant repercussions, as explained before, and a realistic assessment of the associated risk is of great importance.

Induced geoelectric fields

The computation of the electric fields induced by magnetic field variations during a geomagnetic storm requires a good knowledge of the electrical resistivity of the Earth's crust and mantle. The electrical properties of the lithosphere are calculated through a passive electromagnetic geophysical method, the magnetotelluric (MT) method.

The MT method is based on simultaneous measurements of the variations of the natural electric E and magnetic B fields at the surface of the Earth, in periods ranging from $\approx 10^{-3}$ to $\approx 10^{5}$ s. The physical processes responsible for the signal in this period range are the thunderstorm activity and the interaction between the solar wind and the Earth's magnetosphere.

The MT method assumes a linear relationship between the electric and magnetic fields, defined by the impedance tensor ($\mathbb{Z}$). It is a 2 x 2 complex tensor that takes the following form:

$$\begin{bmatrix} E_x \\ E_y \end{bmatrix} = \begin{bmatrix} \mathbb{Z}_{xx} & \mathbb{Z}_{xy} \\ \mathbb{Z}_{yx} & \mathbb{Z}_{yy} \end{bmatrix} \begin{bmatrix} B_x/\mu_0 \\ B_y/\mu_0 \end{bmatrix} \quad (1)$$

where μ_0 is the magnetic permeability of free space (e.g. Simpson & Bahr, 2005).

The tensor $\mathbb{Z}$ is used to chart the subsurface in terms of the apparent resistivity (ρ_a) and the impedance phase (φ) tensors.

The main purpose of geophysical studies is, in general, to provide information on the Earth subsurface. When using the MT method for this purpose, the tensor $\mathbb{Z}$ is inverted in order to estimate the subsurface electrical resistivity distribution. However, equation (1) can also be used to infer the electric fields induced by geomagnetic storms, in a region where the electrical resistivity distribution is known. Therefore, in this application, the MT resistivity model is used to predict the Earth electromagnetic response to geomagnetic storms. This is made through the application of forwarding modelling instead of an inversion.

Conductivity model of the southern Portuguese region

As an illustrative example, let us consider a simplified conductivity model based on studies of the lithosphere in the south of Portugal, inland (Almeida et al., 2005; Da Silva et al., 2007; Alves Ribeiro, 2018) and in the nearby portion of the ocean (Monteiro Santos et al., 2003). It is essential to consider the ocean in the model, as several authors have demonstrated that deep ocean can affect both MT

impedance tensor and the geomagnetic transfer function (Parkinson, 1959; Mackie, 1988; Monteiro Santos et al., 2001) due to the sharp contrasts of conductivity. Therefore, it is expected that the Atlantic Ocean and the Mediterranean Sea can cause a significant “coast effect” (an amplification of the induced electric field perpendicularly to the coastline). Considering the ocean and inland as two distinct 1D resistivity model produces a final 3D model. From this model (Fig. 6), impedance tensor at some sites were calculated and shown in figure 7. Using this impedance tensor the electromagnetic earth response to the geomagnetic storm was estimated (Fig. 8).

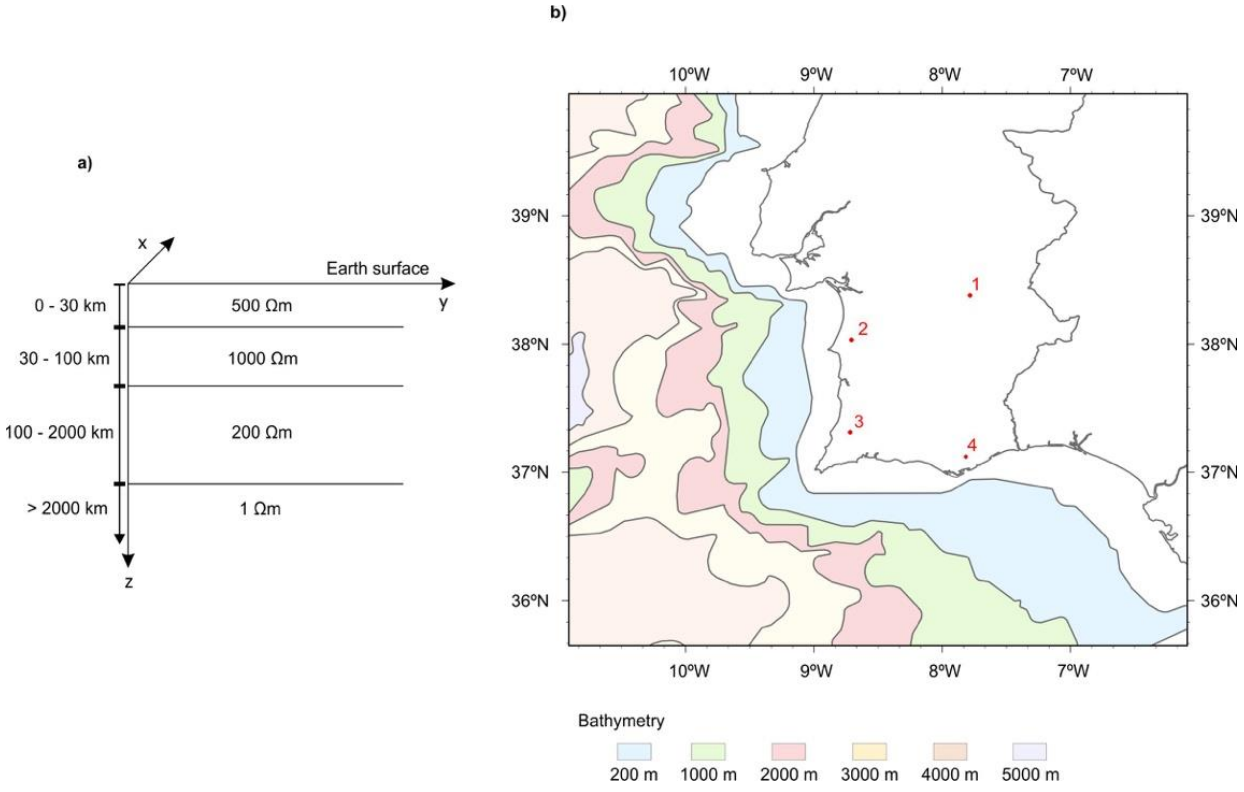

Figure 6 - 3D simplified conductivity model. a. Depth distribution of the electrical resistivity at mainland. b. Bathymetry model used to introduce sea-land discontinuities.

At surface boundaries between regions with sharp conductivity contrasts, as the sea-land boundaries, the continuity condition of the normal electric currents yields that the relatively high conductivity of the sea (0.3 Ω.m) must be balanced by an increase of the inland electric field component perpendicular to the coast. The increase of E_y close to the western coast and E_x close to the southern coast is known as coast effect (e.g. Parkinson, 1959; Mareschal et al., 1987; Monteiro Santos et al., 2001) and is simulated by our conductivity model (see Fig. 6).

Charts of induced geoelectric fields in the southern Portuguese region

Given the size of the Portuguese mainland (on which Coimbra occupies a central position) and the large similarities between the geomagnetic observations recorded at COI and other Iberian

geomagnetic observatories as SPT (San Pablo-Toledo), it was assumed that COI observations provide a good description of the geomagnetic variability taking place over the whole territory covered by the Portuguese transmission power network. Here, we present results concerning the geomagnetic storm on the 7th October 2015, caused by an enhancement of the solar wind. During this event, a disturbance storm time (Dst) index of -124 nT was registered, which is used as a proxy for the equatorial ring current effects. Fig. 8 displays the corresponding geomagnetic field variations recorded at COI. Likewise, Figure 8 also shows the horizontal electric field components induced at the four locations marked out in figure 6. Near the coast, there is an enhancement of the induced electric field in the direction perpendicular to the coastline (coast effect) due to the sudden discontinuity in resistivity in the transition between dry land and the ocean.

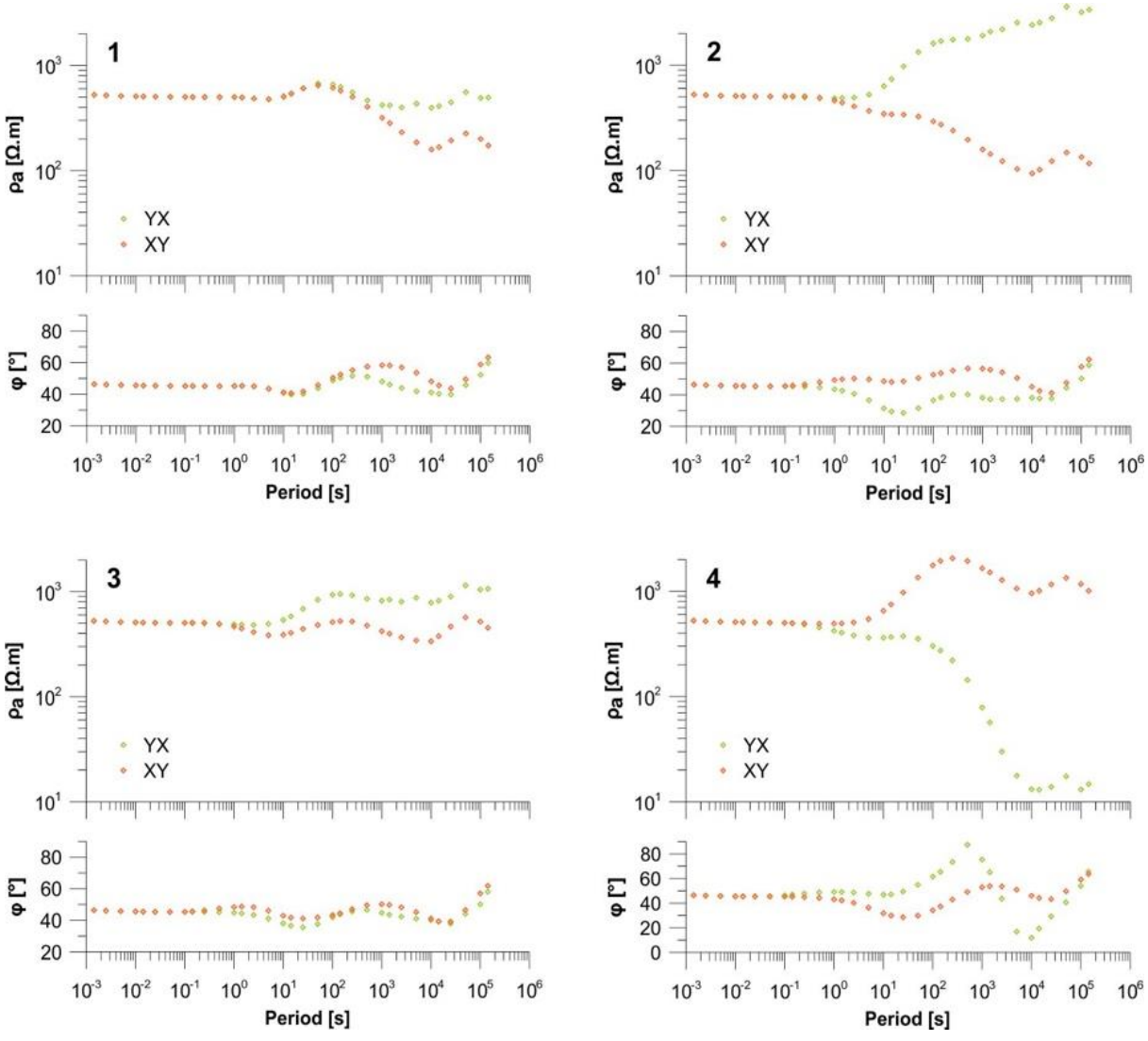

Figure 7 - Apparent resistivity and impedance phase curves, for synthetic MT soundings located in regions of distinct electrical behaviour. The four MT soundings represented correspond to the red dots in figure 6.

Figure 9 shows charts of the induced electric field over the southern Portuguese region, where the coast effect is clearly seen.

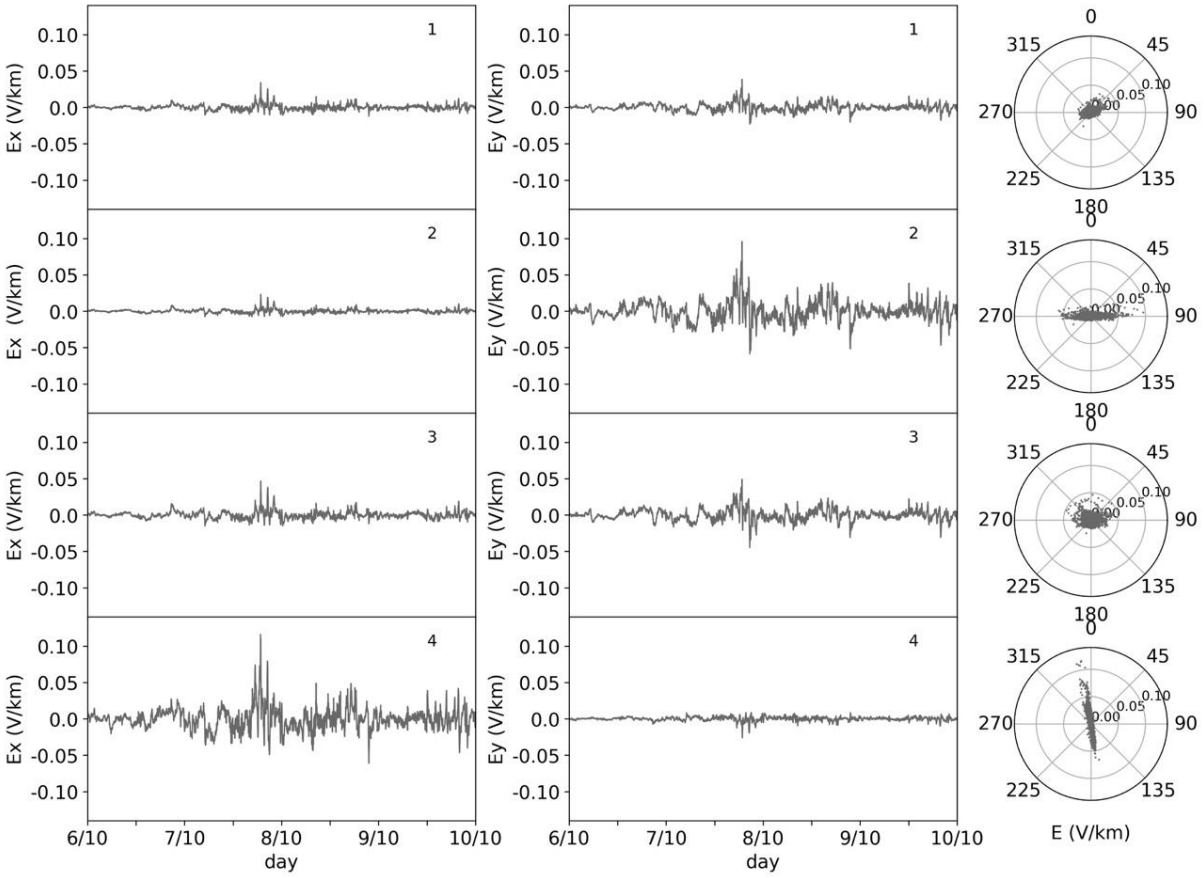

Figure 8 - Induced geoelectric fields in the northward (left) and eastward (middle) directions during the 7th October 2015 storm for the four red points displayed in figure 6. Right: polar plots of the induced geoelectric field.

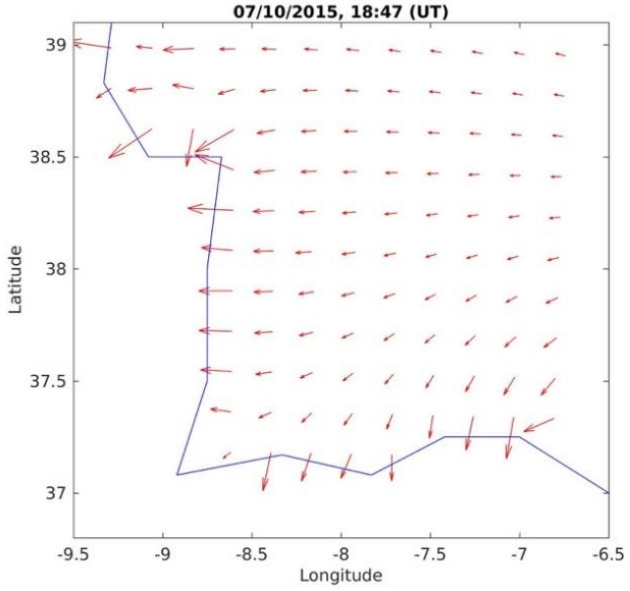

Figure 9 - Chart of the electric field induced in the Southwest of the Iberian Peninsula at 18 h:47 min on the 7th October 2015 [Source: Francisco, 2020].

Computing GICs in HV power networks

The frequencies associated with GIC fluctuations are considerably smaller than the frequency of AC power networks (50Hz in Portugal). Consequently, GICs can be treated as quasi-direct currents. Due to this fact, the calculation of GIC intensities is carried out through the resolution of an electric circuit problem taking only into account resistive impedances. (Lehtinen & Pirjola, 1985).

Applying Ohm's and Kirchhoff's laws to the power network circuit according to Lehtinen & Pirjola (1985) is known as the LP method. It amounts to solve the matrix equation:

$$I = (1 + YZ)^{-1}J \tag{2}$$

For the column vector I, whose elements are GIC intensities through the earthing resistances, at different substations. In addition, 1 is the unit matrix, *Y* is the network admittance matrix whose elements are computed from power line resistances, *Z* is the earthing impedance matrix having the substations' earthing resistances at the diagonal and *J* is the column vector with perfect earthing currents, computed from the induced electric field. The size of column vectors I and J, as well as of square matrices 1, Y and Z in equation (2), are determined by the total number N of nodes in the network.

The computation of the network admittance and the earthing impedance matrices (Eq. 1) requires the following information from the grid: location of the substations and their grounding resistances, the characterisation of the transformers in each substation (amount and type of transformers, winding resistance values for higher and lower voltage windings), the length and line resistances of the transmission lines. Moreover, it is also required to know the number of lines between substations and the type of polyphase system used (i.e. the number of phases of the power system) as these have a direct impact on the amount of current travelling between substations.

Notice that the grounding resistance at each substation is one of the network parameters with the most impact on the computation of GICs (Pirjola, 2008; Zheng et al., 2013). Indeed, lower (larger) grounding resistances mean that larger (lower) currents can flow through the substation grounding connection.

Once the circuit parameters are known, equation (1) can be solved. Currently, there are different numerical codes for the computation of GICs that are available, such as the one computed by Blake et al. (2018) or GEOMAGICA by Bailey et al. (2017)[1] benchmarked against the scripts used by Horton et al. (2012) and Richardson & Beggan (2017).

The southern Portuguese HV power network

To illustrate the effect of a geomagnetic storm on a power system network, we solved the circuit equations (Eq. 2) for the October 2015 storm and the national power network to the south of Palmela

[1] Available in https://github.com/geomagpy/GEOMAGICA.

(shown in Fig. 10), since we presently lack a conductivity model for the North. To the south of Palmela there are 20 substations, where GICs enter/leave the power network through the transformer station's grounding. Two tension levels must be considered, 150 kV (LV) and 400 kV (HV), the two galvanically connected through common earthing at substations and through autotransformer common windings, where these kind of transformers are present.

The required information on the circuit parameters has been obtained in the framework of a collaboration with the national power network operator, REN (Redes Energéticas Nacionais, SGPS, S.A.), that provided the grid parameters as transmission lines, transformer coils and earthing resistances, as well as information on the kind and number of transformers in each substation (Alves Ribeiro et al., 2020). This sort of information is critical to obtain realistic GIC estimations.

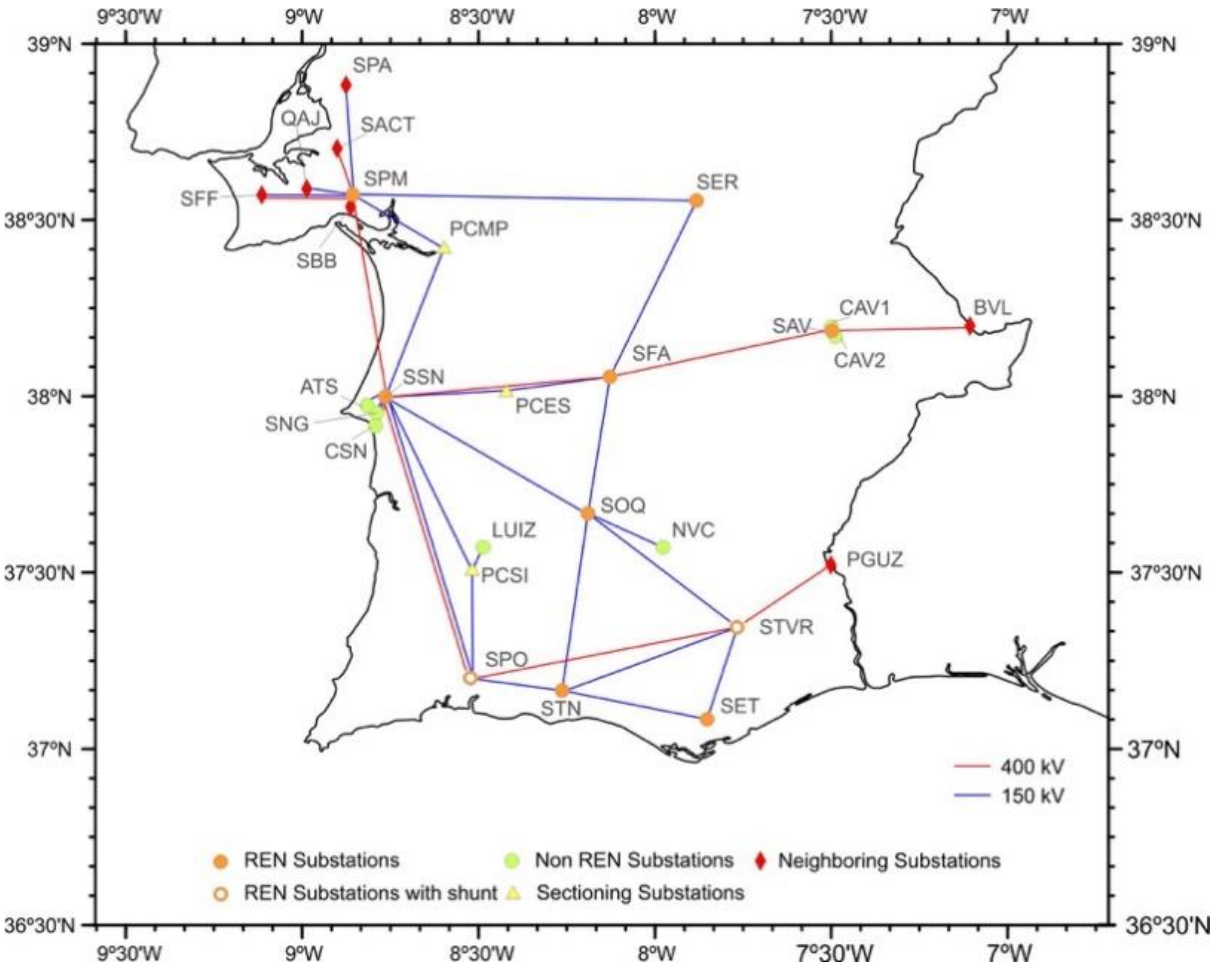

Figure 10 - Southern Portuguese High Voltage power network.

Estimated GICs in the southern Portuguese power network

When no geophysical data is available, but the power network parameters are known, it is still possible to perform sensitivity tests to the network. For instance, assuming the induced electric field is

uniform (generally a 1V/km field) one can determine which substations are more prone to high GICs or how variations in different network parameters affect the GIC estimation (Pirjola, 2008). Let us call α_i and β_i the computed GICs at substation i, when the induced electric field is 1 V/km northward and eastward, respectively. Then, the GIC occurring at the same substation i when the induced E-field is uniform with 1 V/km and making an arbitrary angle θ with the geographic North, is obtained from α_i and β_i through (Boteler, 2013):

$$GIC_i = \alpha_i \cos\theta + \beta_i \sin\theta \quad (3)$$

The peak value for that substation and within the assumption of a uniform E-field of 1 V/km, has amplitude $(\alpha_i^2 + \beta_i^2)^{1/2}$ and is obtained when the horizontal E field is oriented along the direction given by $\arctan(\beta_i / \alpha_i)$. This is shown in figure 11 for substation SET in the South (Alves Ribeiro et al., 2020).

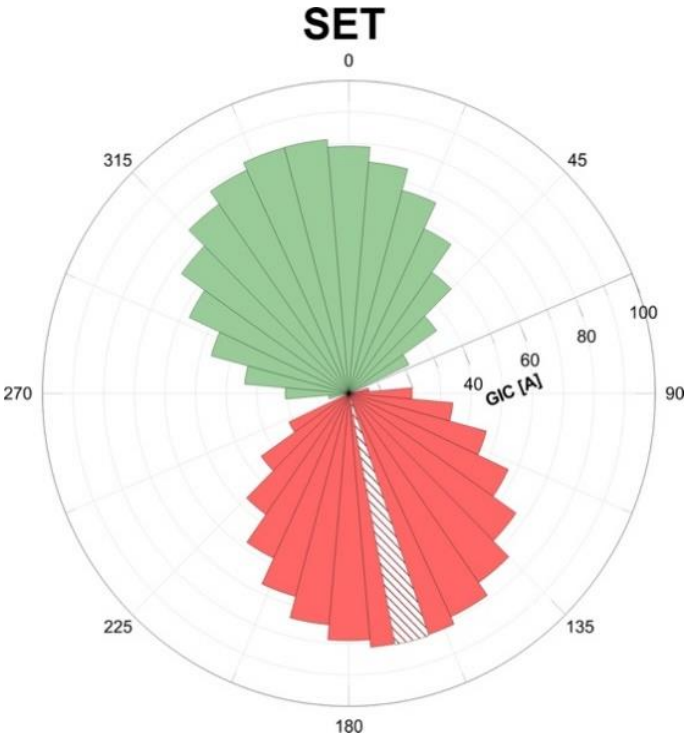

Figure 11 - Directional sensitivity for substation SET. The highest GIC value and preferential orientation for SET substation are represented in backward slash.

Applying this same procedure to each substation in the power network, it is possible to infer the electric field orientation to which each substation is most sensitive (Fig. 12).

A more realistic GIC estimation can be obtained, using geoelectric induced fields computed from an observed geomagnetic storm and a data-based conductivity model. This has been done by solving equation (1) for the 7th October 2015 geomagnetic storm and using the obtained geoelectric fields together with the conductivity model for the southern Portuguese region, to compute the electric field path integrals required to solve equation (2). Results are shown in figure 13 for some of the Portuguese power network substations. One can notice that some of the largest GICs occur at substations near the coast, for which the most favourable direction in figure 12 is approximately

perpendicular to the coastline. This is a result from both the coast effect expected near the coastline and the geometric properties of the grid (edge effect).

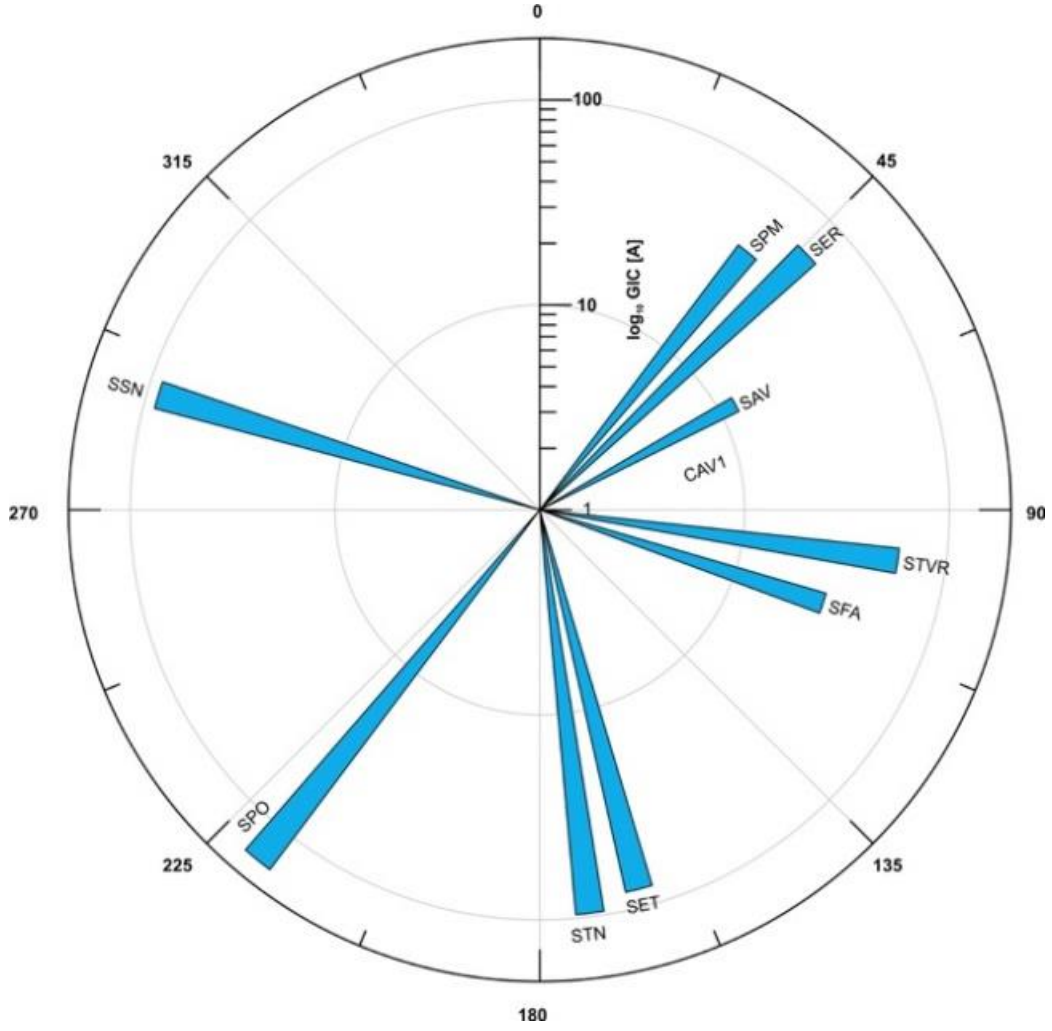

Figure 12 - For a subgroup of substations in figure 10. The orientation of the uniform induced electric field that would produce the highest GIC, and the corresponding GIC amplitude.

Further refinements to the model

The power network information is incomplete since the substations at the edge of the studied network are in fact connected to other substations further north or in Spain. The missing information can significantly affect the GIC results, in particular for those edge substations. This kind of flaw can be partially solved using equivalent circuits (Boteler et al., 2013), where a more or less complex circuit extending north or inside Spain is modelled as a simpler circuit that does not require the complete information on the circuit parameters of the former one.

Furthermore, guard lines can be included as possible paths for GICs. At the top of the power towers that support the transmission lines, there are also, in general, two additional cables running along the power line. These are called guard lines. Their purpose is not to carry electricity to our

homes but instead protect the transmission lines from electrical discharges. Those lines are grounded at the transformer substations and at towers footings, providing further circuits where GICs can flow. For a more accurate GIC estimation, they need to be taken into account in calculations (Liu et al., 2020).

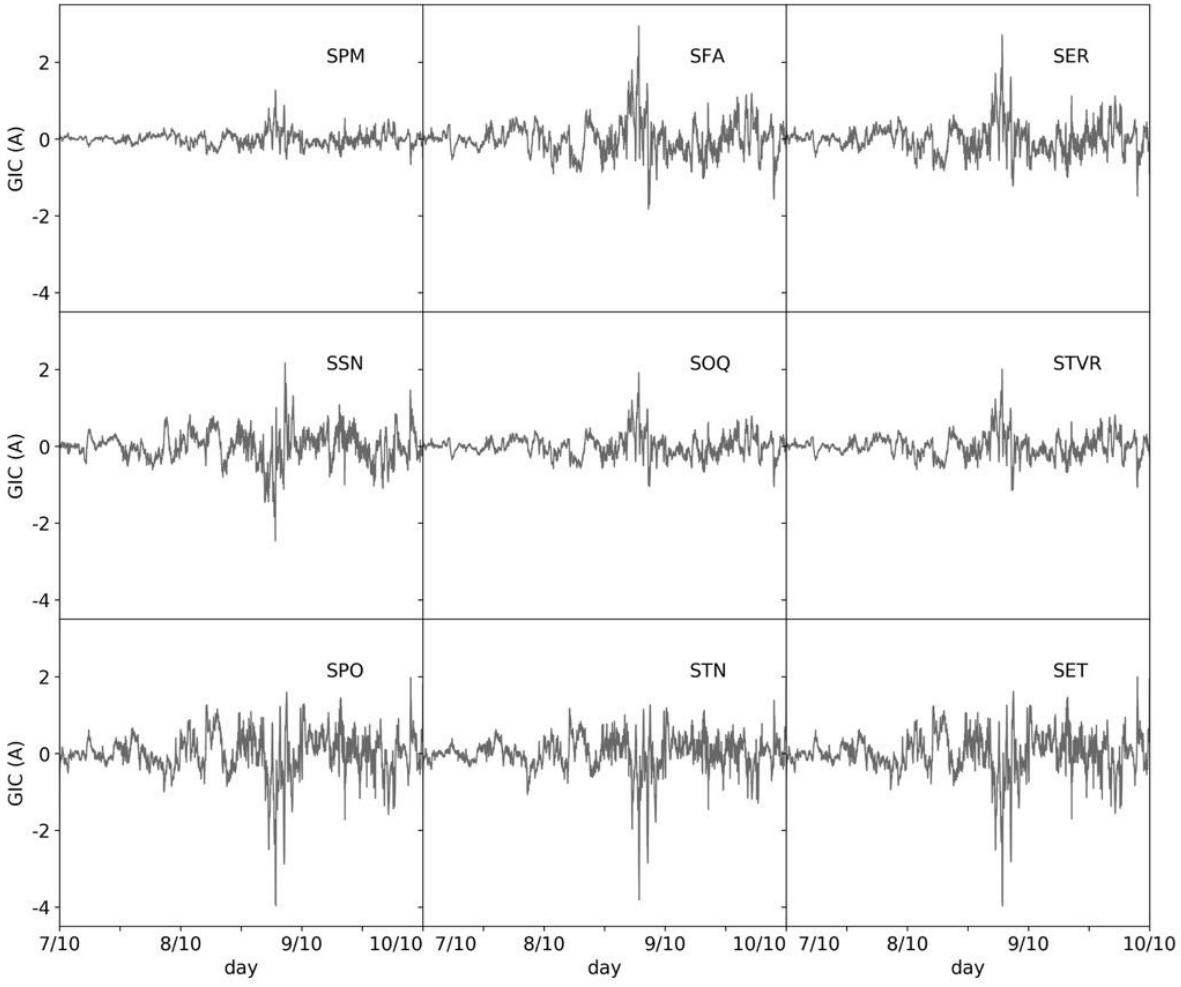

Figure 13 - GICs flowing to (positive) or from (negative) Earth at some substations from the southern Portuguese high voltage power network, during the 7th October 2015 storm.

Concluding remarks

In this article, all different steps required to compute GICs on transmission power networks were presented and shortly discussed. We are presently able to produce estimates for GICs flowing through the earthing resistances, at substations of the southern Portuguese power network operated by REN. However, any model must be tested comparing predictions against measurements. Our study has made it possible to identify some substations in the southern region that are most sensitive to geomagnetic storms. Within the framework of our project (MAG-GIC: PTDC/CTA-GEO/31744/2017), we plan to install an open-loop Hall effect current transducer at one of these substations, in order to

achieve long period logging of GICs data. We expect in this way, to contribute to the decision-making process which is required to prevent power grid failures, but also to use these data to directly test and optimize simulation models and indirectly learn about source magnetospheric currents that flow well above.

Acknowledgements: This study is funded by national funds through FCT (Foundation for Science and Technology, I.P.), under the project MAG-GIC: PTDC/CTA-GEO/31744/2017. CITEUC is funded by National Funds through FCT - Foundation for Science and Technology (project: UID/MULTI/00611/2020). IDL is funded by FCT under project UIDB/50019/2020. We acknowledge the collaboration with REN (Rede Elétrica Nacional), for providing information on the network parameters. This work used the SWMF/BATS-R-US tools developed at the University of Michigan. We are grateful to N. Tsyganenko for making his codes easily available to the scientific community.

References

Almeida, E., Monteiro Santos, F., Mateus, A., Heise, W., & Pous, J. (2005). Magnetotelluric measurements in SW Iberia: New data for the Variscan crustal structures. *Geophysical research letters*, *32*(8), L08312.

Alves Ribeiro, J. (2018). *Magnetotelluric studies in detecting an old suture zone and major crustal scale shear zones (Iberia).* PhD thesis, University of Lisbon, Lisbon.

Alves Ribeiro, J., Pinheiro, F. J. G., & Pais, M. A. (2020). Geomagnetically induced currents in the South of Portugal. *Space Weather* (submitted).

Amory-Mazaudier, C., (2009). Electric current systems in the earth's environment. *Nigerian Journal of Space Research*, *8*, 178-255.

Bailey, R. L., Halbedl, T. S., Schattauer, I., Römer, A., Achleitner, G., Beggan, C. D., & Leonhardt, R. (2017). Modelling geomagnetically induced currents in midlatitude central Europe using a thin-sheet approach. *Annales Geophysicae*, *35*, 751-761.

Blake, S. P., Gallagher, P. T., Campanya, J., Hogg, C., Beggan, C. D., Thomson, A. W. P., & Bell, D. (2018). A detailed model of the Irish High Voltage Power Network for simulating GICs. *Space Weather*, *16*(11), 1770-1783.

Boteler, D. (2013). The use of linear superposition in modelling geomagnetically induced currents. In *2013 IEEE Power & Energy Society general meeting* (p. 5). Vancouver: Power & Energy Society.

Boteler, D., Lackey, A., Marti, L., & Shelemy, S. (2013). Equivalent circuits for modelling geomagnetically induced currents from a neighbouring network. In *2013 IEEE Power & Energy Society general meeting* (p. 5). Vancouver: Power & Energy Society.

Castillo, Y., Pais, M. A., Fernandes, J., Ribeiro, P., Morozova, A.L., & Pinheiro, F. J. G. (2017). Geomagnetic activity at Northern Hemisphere's mid-latitude ground stations: How Much can be

explained using TS05 model. *Journal of Atmospheric and Solar-Terrestrial Physics*, *165-166*, 38-53.

Chapman, S., & Bartels, J. (1940). *Geomagnetism*. Oxford: Oxford University Press.

Da Silva, N. V., Mateus, A., Monteiro Santos, F. A., Almeida, E., & Pous, J. (2007). 3-d electromagnetic imaging of a palaeozoic plate-tectonic boundary segment in SW Iberian Variscides (S. Alentejo, Portugal). *Tectonophysics*, *445*(1-2), 98-115.

Eastwood, J. P., Biffis, E., Hapgood, M. A., Green, L., Bisi, M. M., Bentley, R. D., … Burnett, C. (2017). The economic impact of Space Weather: Where do we stand? *Risk Analysis*, *37*, 206.

Finlay, C. C., Lesur, V., Thébault, E., Vervelidou, F., Morschhauser, A., & Shore, R. (2017). Challenges handling magnetospheric and ionospheric signals in internal geomagnetic field modelling (2017). *Space Science Review, 206***,** 157-189.

Francisco, C. F. (2020). *Preliminary study of the sensibility to geomagnetic storms of the power network substations in Portugal south region.* MSc thesis, University of Coimbra, Coimbra.

Ganushkina, N. Y., Liemohm, M. W., & Dubyagin, S. (2018). Current systems in the Earth's magnetosphere. *Reviews of Geophysics*, *56*(13), 309-332.

Glocer, A., Fok, M., Meng, X., Toth, G., Buzulukova, N., Chen, S., & Lin, K. (2013). CRCM + BATS-R-US two-way coupling. *Journal of Geophysical Research (Space Physics)*, *118*(4), 1635-1650.

Gonzalez, W. D., Joselyn, J. A., Kamide, Y., Kroeh, H. W. l, Rostoker, G., Tsurutani, B. T., & Vasyliunas, V. M. (1994). What is a geomagnetic storm*? Journal of Geophysical Research*, *99* (A4), 5771-5792.

Horton, R., Boteler, D., Overbye, T. J., Pirjola, R., & Dugan, R. C. (2012). A test case for the calculation of geomagnetically induced currents. *IEEE Transactions on Power Delivery*, *27*(4), 2368-2373.

Hulot, G., Sabaka, T., Olsen, N., & Fournier, A. (2015). The present and future geomagnetic field. In G. Schubert (Ed.), *Treatise on Geophysics* (2nd ed.) (pp. 33-78). Amsterdam, San Diego: Elsevier, Academic Press.

Koskinen, H. E. J. (2011). *Physics of space storms from the solar surface to the Earth*. Berlin, Heidelberg: Springer-Verlag Publishing.

Lehtinen, M., & Pirjola, R. (1985). Currents produced in earthed conductor networks by geomagnetically-induced electric fields. *Annales geophysicae, 3*, 479-484.

Liu, C., Boteler, D. H., & Pirjola, R. J. (2020). Influence of shield wires on geomagnetically induced currents in power systems. *International Journal of Electrical Power & Energy Systems*, *117*, 105653.

Mackie, R., & Madden, T. (1993), Three-dimensional magnetotelluric inversion using conjugate gradients, *Geophysical Journal International*, *115*(1), 215-229.

Mandea, M., Holme, R., Pais, A., Pinheiro, K., Jackson, A., & Verbanac, G. (2010), Geomagnetic jerks: Rapid core field variations and core dynamics. *Space Science Review*, *155*, 147-175.

Mareschal, M., Vasseur, G., Srivastava, B., & Singh, R. (1987). Induction models of southern India and the effect of off-shore geology. *Physics of the Earth and planetary interiors*, *45*(2), 137-148.

Maunder, E. W., (1905). The solar origin of terrestrial magnetic disturbances. *Astrophysical Journal*, *21*, 101.

Molinski, T. S. (2002). Why utilities respect geomagnetically induced currents. *Journal of Atmospheric and Solar-Terrestrial Physics*, *64*(16), 1765-1778.

Monteiro Santos, F. A., Nolasco, M., Almeida, E. P., Pous, J., & Mendes-Victor, L. A. (2001). Coast effects on magnetic and magnetotelluric transfer functions and their correction: application to mt soundings carried out in SW Iberia. *Earth and Planetary Science Letters*, *186*(2), 283-295.

Monteiro Santos, F. A., Soares, A., Nolasco, R., Rodrigues, H., Luzio, R., Palshin, N., & Team, I.-D. (2003). Lithosphere conductivity structure using the cam-1 (Lisbon-Madeira) submarine cable. *Geophysical Journal International*, *155*(2), 591-600.

Morozova, A. L., Ribeiro, P., & Pais, M. A. (2014). Correction of artificial jumps in the historical geomagnetic measurements of Coimbra Observatory, Portugal. *Annales geophysicae*, *32*, 19-40.

Oughton, E. J. (2018). The economic impact of critical national infrastructure failure due to Space Weather. In D. Benouar (Ed.), *Oxford Research Encyclopedia of Natural Hazard Science.* Oxford: Oxford University Press.

Oughton, E. J., Hapgood, M., Richardson, G. S., Beggan, C. D., Thomson, A. W. P., Gibbs, M., … Horne, R. B. (2019). A risk assessment framework for the socioeconomic impacts of electricity transmission infrastructure failure due to Space Weather: An application to the United Kingdom, *Risk Analysis*, *29*, 1022.

Pais, M. A., & Miranda, J. M. A. (1995). Secular variation in Coimbra (Portugal) since 1866. *Journal of Geomagnetism and Geoelectricity*, *47*, 267-282.

Parkinson, W. (1959). Directions of rapid geomagnetic fluctuations. *Geophysical Journal International*, *2*(1), 1-14.

Pirjola, R. (2002). Review on the calculation of surface electric and magnetic fields and of geomagnetically induced currents in ground-based technological systems. *Surveys in geophysics*, *23*(1), 71-90.

Pirjola, R. (2008). Study of effects of changes of earthing resistances on geomagnetically induced currents in an electric power transmission system. *Radio Science*, *43*(1), 1-13.

Pulkkinen, A., Bernabeu, E., Eichner, J., Beggan, C., & Thomson, A. W. P. (2012). Generation of 100-year geomagnetically induced current scenarios. *Space Weather*, *10*(4), S04003.

Ribeiro, P., & Pais, M. A. (2004). An account of geomagnetic observations in Coimbra since 1952. In *Book of abstracts of the International workshop: Challenges for Geomagnetism, Aeronomy and Seismology in the XXI Century* (p. 91). Roquetes, Tarragona: Observatório del Ebro.

Richardson, G. S., & Beggan, C. D. (2017). *Validation of geomagnetically induced current modelling code (Tech. Rep. No. IR/17/009)*. Edinburgh: British Geological Survey.

Schrijver, C. J., Dobbins, R., Murtagh, W., & Petrinec, S. M. (2014). Assessing the impact of space weather on the electric power grid based on insurance claims for industrial electrical equipment. *Space Weather*, *12*, 487.

Simpson, F., & Bahr, K. (2005). *Practical magnetotellurics*. Cambridge: Cambridge University Press.

Torta, J. M., Marcuello, A., Campanyà, J., Marsal, S., Queralt, P., & Ledo, J. (2017). Improving the modeling of geomagnetically induced currents in Spain. *Space Weather*, *15*, 691.

Tsyganenko, N. A., & Sitnov, M. I. (2005). Modeling the dynamics of the inner magnetosphere during strong geomagnetic storms. *Journal of Geophysical Research (Space Physics)*, *110*(A3), A03208.

Yamazaki, Y., & Maute, A. (2017). Sq and EEJ - a review on the daily variation of the geomagnetic field caused by ionospheric dynamo currents. *Space Science Reviews*, *206*(1-4), 299-405.

Zheng, K., Boteler, D., Pirjola, R. J., Liu, L.-g., Becker, R., Marti, L., & Guillon, S. (2013). Effects of system characteristics on geomagnetically induced currents. *IEEE Transactions on Power Delivery*, *29*(2), 890-898.